Pore Topology of the Hyperpolarization-Activated Cyclic Nucleotide-Gated Channel from Sea Urchin Sperm

Paola Roncaglia, Pavel Mistrík, and Vincent Torre

Scuola Internazionale Superiore di Studi Avanzati and Istituto Nazionale di Fisica della Materia Unit, 34014 Trieste, Italy

ABSTRACT   The current flow through hyperpolarization-activated cyclic nucleotide-gated (HCN) channels, referred to as I_h, plays a major role in several fundamental biological processes. The sequence of the presumed pore region of HCN channels is reminiscent of that of most known K^+-selective channels. In the present work, the pore topology of an HCN channel from sea urchin sperm, called SpHCN, was investigated by means of the substituted-cysteine accessibility method (SCAM). The I_h current in the wild-type (w.t.) SpHCN channel was irreversibly blocked by intracellular Cd^{2+}. This blockage was not observed in mutant C428S. Extracellular Cd^{2+} did not cause any inhibition of the I_h current in the w.t. SpHCN channel, but blocked the current in mutant channels K433C and F434C. Large extracellular anions blocked the current both in the w.t. and K433Q mutant channel. These results suggest that 1) cysteine in position 428 faces the intracellular medium; 2) lysine and phenylalanine in position 433 and 434, respectively, face the extracellular side of the membrane; and 3) lysine 433 does not mediate the anion blockade. Additionally, our study confirms that the K^+ channel signature sequence GYG also forms the inner pore in HCN channels.

INTRODUCTION

The I_h current, activated after the hyperpolarization of an excitable membrane, controls fundamental biological processes such as the heart beat (DiFrancesco, 1993; Brown and Ho, 1996) and the generation of neuronal rhythmic activity (Halliwell and Adams, 1982; Pape, 1996). The I_h current is activated at membrane voltages around -50 mV, is carried by a mixture of Na^+ and K^+ ions (Wollmuth and Hille, 1992; Ho et al., 1994), and is powerfully blocked by Cs^+ (Fain et al., 1978). The voltage dependency of the activation of I_h is modulated by cyclic nucleotides, and the ionic channels through which this current flows have been referred to as HCN (hyperpolarization-activated cyclic nucleotide-gated) channels (Clapham, 1998). HCN channels have been recently cloned and their heterologous expression demonstrated by several groups. In vertebrates, channels HCN1–4 have been cloned from brain and heart (Santoro et al., 1997, 1998; Ludwig et al., 1998, 1999; Ishii et al., 1999; Seifert et al., 1999; Shi et al., 1999; Vaccari et al., 1999). In addition, HCN channels were recently cloned from sea urchin sperm (SpHCN; Gauss et al., 1998), the silkmoth (HvHCN; Krieger et al., 1999), and the fruitfly (Marx et al., 1999). Cloned HCN channels have properties very similar to those of native I_h channels. It is not known yet whether native HCN channels are homomeric or heteromeric.

HCN channels are structurally and functionally related to cyclic nucleotide-gated (CNG) channels and to K^+ channels (for a review, see Santoro and Tibbs, 1999). In the primary sequence of all members of this channel superfamily it is possible to identify six putative transmembrane segments,

with the fourth bearing a voltage sensor as in the K^+ channels—although sensitized by hyperpolarization—and a pore region located between the fifth and sixth segments. Similarly to CNG channels, HCN channels have a cyclic nucleotide-binding (CNB) domain in the C-terminus, which has a significant homology with the CNB domain of CNG channels and of other cyclic nucleotide-regulated proteins such as the catabolite activator protein (CAP) from *Escherichia coli* and cAMP- and cGMP-dependent protein kinases (for a review, see Gauss and Seifert, 2000). Given the structural similarity to CNG and K^+ channels, HCN channels are thought to have a tetrameric structure.

High sequence homology among HCN, CNG, and K^+ channels does not prevent the existence of important functional differences. First, the selectivity; while CNG channels do not select among monovalent alkali cations (Capovilla et al., 1983; Fesenko et al., 1985), HCN channels are able to discriminate among them but with a much lower efficiency than that of K^+ channels. Indeed, the I_h current is carried by a mixture of K^+ and Na^+ ions. Second, the gating is also different. While in CNG channels this is almost independent of membrane voltage, HCN channels are opened by membrane hyperpolarization, and K^+ channels are activated by depolarization (for a review on possible models of HCN channel activation, see Santoro and Tibbs, 1999). In summary, HCN channels have almost intermediate properties between CNG and K^+ channels.

The pore region of HCN channels (see Fig. 1 *A*) bears the GYG motif common to the great majority of K^+ channels, but differs in at least two important features. First, while most known K^+ and CNG channels have a negative residue in the extracellular mouth of the channel (aspartate and glutamate, respectively), HCN channels have either a positively charged or a neutral residue at the homologous location: a lysine in SpHCN, an arginine in mHCN2 and hHCN4, an alanine in mHCN1, and a glutamine in mHCN3.

Second, all cloned HCN channels have a cysteine residue where K^+ and CNG channels have a threonine or a serine residue.

In this paper we investigate the topology of the pore of the SpHCN channel from position 428 to 434 by means of the substituted-cysteine accessibility method (SCAM), and the role of the positively charged lysine in position 433. Several of the engineered cysteine mutants did not lead to functional channels, but we were able to study the accessibility and the role of cysteine, lysine, and phenylalanine in position 428, 433, and 434, respectively, indicated by arrows in Fig. 1 A. Our results indicate that residues K433 and F434 face the extracellular side of the membrane. On the contrary, residue C428 faces the cytoplasmic medium and is responsible for the blocking effect of the I_h current from intracellular Cd^{2+}. As a consequence, the inner pore of the SpHCN channel is formed by residues CIGYGK spanning the lipid membrane from the intracellular to the extracellular side and containing the signature GYG of usual K^+ channels. These results also indicate that the pore topology of the SpHCN channel is similar to that of the KcsA K^+ channel (Doyle et al., 1998; Zhou et al., 2001). The role of the positively charged lysine 433, which is located immediately after the selectivity filter GYG, was also studied, with the aim to establish whether this residue is responsible for the "intermediate" ion selectivity of HCN channels. It was found that lysine 433 was neither responsible for this characteristic nor for the modulation of the I_h current by extracellular large anions, as observed in both native (Frace et al., 1992) and expressed (Santoro et al., 1998) HCN channels.

MATERIALS AND METHODS

Molecular biology

The SpHCN clone was mutated using the QuikChange site-directed mutagenesis kit (Stratagene, La Jolla, CA). All mutant clones were sequenced completely with the DNA sequencer LI-COR (4000L) to verify sequence correctness. Wild-type (w.t.) and mutant RNAs were then synthesized in vitro by using the mCAP RNA capping kit (Stratagene).

Oocyte preparation and chemicals

The w.t. or mutant channel cRNAs were injected into *Xenopus laevis* oocytes (Inst. fur Entwicklungsbiologie, Hamburg, Germany). Oocytes were prepared as previously described (Nizzari et al., 1993). Injected eggs were maintained at 18°C in a Barth solution supplemented with 50 μg/ml gentamycin sulfate and containing (in mM): 88 NaCl, 1 KCl, 0.82 $MgSO_4$, 0.33 $Ca(NO_3)_2$, 0.41 $CaCl_2$, 2.4 $NaHCO_3$, 5 TRIS-HCl, pH 7.4 (buffered with NaOH). During the experiments, oocytes were kept in a Ringer's solution containing (in mM): 150 NaCl, 2.5 KCl, 1 $CaCl_2$, 1.6 $MgCl_2$, 10 HEPES-NaOH, pH 7.4 (buffered with NaOH). All reagents were from Sigma Chemicals (St. Louis, MO).

Recording apparatus

HCN currents from excised patches (Hamill et al., 1981) were recorded with a patch-clamp amplifier (Axopatch 200B, Axon Instruments Inc.,

Foster City, CA), 1–5 days after RNA injection, at room temperature (20–22°C). The perfusion system was as previously described (Sesti et al., 1995), allowing complete solution changing within 1 s. Borosilicate glass pipettes had resistances of 3–5 MΩ in symmetrical standard solution. The current traces used for obtaining steady-state current-voltage relations were the difference between currents in the presence and in the absence of 1 mM cAMP. The patch potential was stepped from -100 to $+10$ mV (10 mV steps), from 0 mV. Currents were low-pass filtered at 1 kHz and acquired on-line (at 5 kHz). For data acquisition and analysis, we used pClamp hardware and software (Axon Instruments) and Origin software (Microcal Software, Inc.).

Identification and isolation of I_h current

To measure I_h current, patches of membrane where excised from *Xenopus laevis* oocytes heterologously expressing the SpHCN channel. Currents were measured in both inside- and outside-out patch-clamp configurations (Fig. 1, B and C). In inside-out experiments, the patch pipette contained (in mM): 150 KCl, 10 HEPES, 0.2 EDTA ("standard solution" buffered at pH 7.6 with tetramethylammonium hydroxide). The external solution was the same but supplemented or not with 1 mM cAMP. I_h currents were elicited applying hyperpolarizing steps to the membrane voltage (in most experiments, -100 mV), and were taken as the difference between the current recorded in the presence of cAMP and in its absence. In outside-out experiments, the patch pipette contained the "standard solution" described above. The external solution contained (in mM): 150 KCl, 10 HEPES, 0.2 EDTA. The I_h current activated by stepping the membrane voltage from 0 to $-X$ mV was taken as the sum of the current recordings when the voltage was stepped from 0 to $-X$ mV and from 0 to $+X$ mV.

Application of sulfhydryl-specific reagents

To test the effect of sulfhydryl-specific reagents on SpHCN current, Cd^{2+} was applied from the intra- or extra-cellular side of the membrane. In the inside-out patch-clamp configuration, soon after patch excision, the cytoplasmic face of the plasma membrane was perfused with the same pipette-filling solution supplemented or not with 1 mM cAMP. The Cd^{2+} effect was tested by perfusing the intracellular side of the patch with a standard solution without EDTA (to avoid partial Cd^{2+} chelation; Gordon and Zagotta, 1995) supplemented with 1 mM cAMP and/or 50 μM $CdCl_2$. The only effect of the EDTA withdrawal was the activation of a background offset current due to the well-known presence of Ca^{2+}-dependent Cl^- channels in *Xenopus* oocytes (Miledi and Parker, 1984). Because this current reached the steady state soon after the solution changed, as reported also in previous work (Becchetti and Roncaglia, 2000), we never added any Cl^- channel blockers during these experiments. In outside-out experiments, soon after patch excision, the extracellular face of the plasma membrane was perfused with the same pipette-filling solution deprived of cAMP and supplemented or not with 50 μM $CdCl_2$.

Determination of ionic selectivity

Ionic selectivity was determined in inside-out patches by stepping V_m from a holding potential of 0 mV to -100 mV for 1 s (for the w.t.) and to -120 mV for 200 ms (for mutant channel K433Q) to test values between $+50$ and -60 mV in 10 mV increments, to determine the reversal potential of the tail current. When the patch was excised, the cytoplasmic face of the plasma membrane was perfused with a solution containing (in mM): 50 KCl, 100 XCl, 10 HEPES, 0.2 EDTA and supplemented or not with 1 mM cAMP, where X is potassium, sodium, or lithium. Because mutant K433Q I_h current exhibits rundown, we tested the different ions on separate membrane patches immediately after patch excision. The determination of
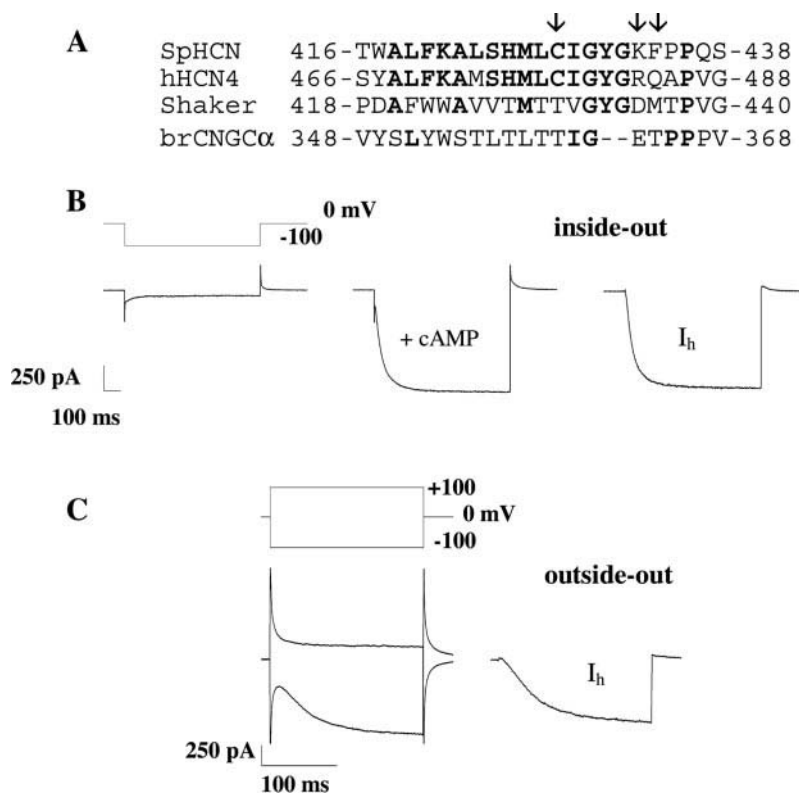
FIGURE 1   Amino acid alignment and I_h current isolation. (*A*) Alignment of the amino acid sequence in the pore region of two HCN channels and two other members of the K^+ channel superfamily. Residues identical to the corresponding positions in SpHCN are in bold characters. Cysteine 428, lysine 433, and phenylalanine 434 in SpHCN are indicated by arrows. From top to bottom: SpHCN: HCN channel from the sperm of the sea urchin *Strongylocentrotus purpuratus* (Gauss et al., 1998); hHCN4: HCN channel from human tissue (Ludwig et al., 1999; Seifert et al., 1999); *Shaker*: K^+ channel encoded by the *Drosophila Shaker b* gene (Pongs et al., 1988); brCNGCα: α-subunit of the CNG channel from bovine rod photoreceptors (Kaupp et al., 1989). (*B* and *C*) Identification of the I_h current. (*B*) Current recordings in an inside-out patch during voltage steps from 0 to -100 mV in the absence (*left*) and in the presence (*middle*) of 1 mM cAMP in the intracellular medium. Voltage steps lasting 1 s. The I_h current (*right*) is taken as the difference of the two traces. (*C*) Current recordings in an outside-out patch during voltage steps from 0 to -100 mV and from 0 to $+100$ mV in the presence of 1 mM cAMP in the extracellular medium, i.e., in the solution filling the patch pipette (*left*). Voltage steps lasting 250 ms. The I_h current (*right*) is taken as the sum of the two traces.

the reversal potential for mutant K433Q occurred in <15 s, during which the rundown of the I_h was only ~10%.

Application of chloride-substituting anions

To determine the effect of the substitution of external chloride with larger anions, current recordings were performed in both inside- and outside-out patch-clamp configurations. The cytoplasmic face of the plasma membrane was perfused in the inside-out configuration with a solution containing (in mM): 150 KX, 10 HEPES, 0.2 EDTA, and supplemented or not with 1 mM cAMP (buffered as above), where X is acetate, glutamate, aspartate, or sulfate. In outside-out experiments, the extracellular face of the excised membrane was perfused with a solution containing (in mM): 150 KX, 10 HEPES, 0.2 EDTA (buffered as above), with X meaning the same as above.

Homology modeling

A homology model of the SpHCN channel pore was constructed using the amino acid sequence alignment in Fig. 1 *A* and the crystallographic coordinates of KcsA (Zhou et al., 2001). The model was generated using

MODELLER (Sali and Blundell, 1993). The final results were displayed using the software package VMD (Humphrey et al., 1996).

RESULTS

Xenopus laevis oocytes were injected with the cRNA of the SpHCN channel. The plasma membrane of uninjected oocytes contains some stretch-activated channels and Ca^{2+}-activated chloride channels, but does not have a significant density of other ionic channels, either activated by voltage and/or by cyclic nucleotides. Therefore, in a Ca^{2+}-free medium the electrical properties of plasma membrane of uninjected oocytes can be described by passive components, such as conductors and capacitors.

Current recordings from inside-out (Fig. 1 *B*) or outside-out (Fig. 1 *C*) membrane patches excised from oocytes injected with the cRNA of the SpHCN channel clearly showed an I_h current in the presence of cAMP in the intracellular side of the membrane patch when the mem-

brane voltage was stepped from 0 to -100 mV. If cAMP was removed from the intracellular medium, the I_h current usually disappeared within one second or so; therefore, I_h currents flowing through HCN channels heterologously expressed in *Xenopus laevis* oocytes can be clearly identified and isolated. These currents have a sigmoidal waveform with a time constant around 60 ms, characteristic of all vertebrate I_h currents (DiFrancesco, 1993; Pape, 1996; for the characterization of the SpHCN w.t. channel heterologously expressed in a different cell system, see Gauss et al., 1998). In inside-out patches, the I_h current was taken as the difference between the current recorded in the presence of cAMP and in its absence (Fig. 1 *B*). In outside-out patches, when the patch pipette contained 1 mM cAMP, the I_h current activated by stepping the voltage from 0 to $-X$ mV was taken as the sum of the current recordings when the voltage was stepped from 0 to $-X$ mV and from 0 to X mV (Fig. 1 *C*).

SpHCN channel pore structure

Extensive mutational analysis was performed on the SpHCN channel pore-forming residues, from 421 to 437, to investigate their physical location and functional properties. Based on an alignment of selected members of the K^+ channel superfamily, depicted in Fig. 1 *A*, several mutant channels were engineered to understand functional differences among HCN-, CNG-, and K^+-selective channels. Those were K421W, Δ(Y431+G432) (in which tyrosine and glycine in position 431 and 432, respectively, were deleted), and Q437P. However, no current was detected in any of these mutants. Subsequently, the physical location of pore-forming residues was addressed. The pore topology of the SpHCN channel was probed by the substituted-cysteine accessibility method (SCAM; Karlin and Akabas, 1998). Here, individual residues are mutated into a cysteine and their intracellular or extracellular accessibility is probed by analyzing the blocking effect of compounds such as Cd^{2+} or MTSET, known to bind to the cysteine sulfhydryl. By using this procedure, the pore topology of a number of ionic channels has been determined (Yellen et al., 1994; Kurz et al., 1995; Krovetz et al., 1997; Kubo et al., 1998; Becchetti et al., 1999). In our case, the following mutants were engineered: I429C, G430C, Y431C, G432C, K433C, and F434C. Additionally, the accessibility of the cysteine residue, which naturally occurs in all HCN channels cloned so far, was also addressed (position 428 in SpHCN). While no I_h current was detected for mutants I429C, G430C, Y431C, and G432C, reliable I_h currents were observed in mutants K433C and F434C. Therefore, it was possible to assess the physical location of residues C428, K433, and F434.

The effect of Cd^{2+} from the extracellular side of the membrane was analyzed for w.t., K433C, and F434C channels, in the outside-out configuration, with the patch pipette containing 1 mM cAMP. As shown in Fig. 2 *A*, extracellular Cd^{2+} application does not significantly block the w.t. I_h current, and has the only effect of slowing down its kinetics. In fact, the analysis of the *I-V* relations, shown in Fig. 2 *F*, indicates that the major effect of extracellular Cd^{2+} is to shift the activation of the I_h current toward more negative voltages by $\sim$5 mV. As for the mutant channel K433C, the I_h current flowing through it was powerfully blocked by extracellular Cd^{2+} application (Fig. 2 *B*). However, a clear I_h current was only observed in outside-out patches excised from cells that were kept in a solution containing 2 mM DTT as a reducing agent (two occasions of several attempts with at least 20 oocytes). The presence of DTT in the medium seems important in preventing the formation of sulfhydryl bonds between nearby cysteines in position 428 (see also Becchetti and Gamel, 1999). When oocytes injected with the cRNA of mutant channel K433C were kept in the usual extracellular medium (see Methods), I_h currents were never observed, neither in inside- nor in outside-out patches.

An I_h current was also observed in mutant channel F434C (with 2 mM DTT in the incubation solution). In this case, too, the I_h current was powerfully and irreversibly reduced by the addition of 50 μM Cd^{2+} to the extracellular medium, as shown in Fig. 2 *C* (10 patches from 5 oocytes). These results indicate that lysine in position 433 and phenylalanine in position 434 lie at the extracellular side of the channel pore.

The effect of Cd^{2+} on the w.t. I_h current was also analyzed from the intracellular side of the membrane. As shown in Fig. 2 *D*, a 30-s application of 50 μM Cd^{2+} powerfully blocked w.t. I_h current when applied on the cytoplasmic face of the membrane patch. Intracellular Cd^{2+} application had no blocking effect on the mutant channel C428S (Fig. 2 *E*), where cysteine 428 is substituted with a similar residue, serine. These results indicate that the cysteine in position 428 of the SpHCN channel is accessible to intracellular but not extracellular Cd^{2+}, and is therefore located on the cytoplasmic side of the membrane.

Properties of the cysteine 428 ring

The physical properties of the naturally occurring cysteine in position 428 of the SpHCN channel were further analyzed, given the highly conserved nature of this residue within the HCN channel family (see Fig. 1 *A*). Namely, the location of C428 within the intracellular mouth of the pore was assessed. Given the presumed quaternary structure of the channel, the four C428 residues form a ring within the mouth. A mutual proximity of the ring members can be determined from their ability to form a disulfide bridge in a nonreducing environment (Krovetz et al., 1997). A mild oxidative agent, copper phenanthroline (Cu/P), was added to the intracellular medium. Its ability to promote the formation of disulfide bridges, leading to channel blockage, was tested. As shown in Fig. 3 *A*, 1.5:5 μM Cu/P applied
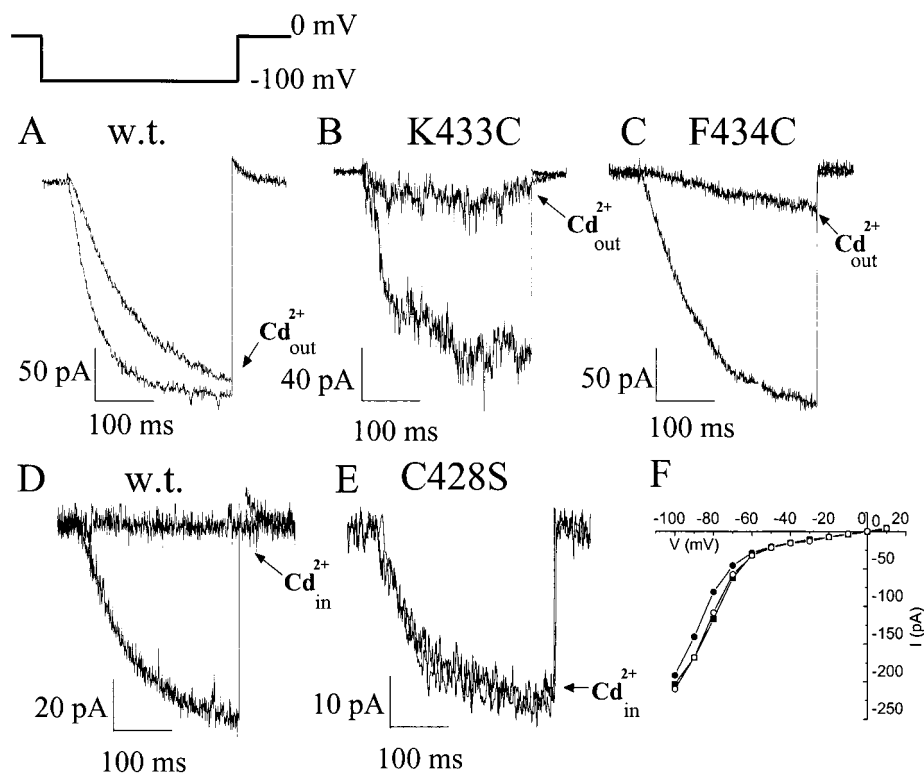
FIGURE 2 Pore residue accessibility to sulfhydryl-specific reagents. (A–C) Effect of extracellularly applied Cd^{2+} on the I_h current of w.t. and mutant SpHCN channel. I_h currents were elicited as in Fig. 1 C in the presence of 1 mM cAMP in the pipette-filling solution. The effect of a 30-s 50 μM $CdCl_2$ application is shown as a superimposed trace (Cd^{2+} out). (A) Extracellular Cd^{2+} has little effect on w.t. I_h current. Traces are representative of five experiments. (B and C) Extracellular Cd^{2+} powerfully blocks I_h current in both mutant channels K433C (B) and F434C (C). Traces are representative of 2 (K433C) and 10 (F434C) experiments. (D and E) Effect of intracellularly applied Cd^{2+} on the I_h current of w.t. and mutant SpHCN channels. I_h currents were elicited as in Fig. 1 B, in the presence of 1 mM cAMP in the bath solution. The effect of a 30-s 50 μM $CdCl_2$ application is shown as a superimposed trace (Cd^{2+} in). Traces are representative of four experiments. (D) Intracellular Cd^{2+} powerfully blocks w.t. I_h current. (E) Intracellular Cd^{2+} has no effect on the I_h current of mutant channel C428S. (F) Extracellular Cd^{2+} shifts the I_h current activation curve by only ~5 mV. Current-voltage (I/V) relationship taken from B. Control (before Cd^{2+} application), *filled triangles*; during Cd^{2+} application, *filled circles*; recovery (after Cd^{2+} application), *empty circles*.

intracellularly induced blockage of the w.t. I_h current within <1 min (five recordings from two oocytes). This current blockage was not reversible and exhibited exponential decay kinetics with a time constant of 25 ± 4 s (Fig. 3 B, no blockage was observed in the absence of Cu/P). When the same experiment was performed with the C428S mutant channel, only a partial blockage was observed (Fig. 3 C; no blockage was observed in the absence of Cu/P). Furthermore, the decay kinetics of the current in C428S was much slower than for the w.t. channel (time constant of 300 ± 50; Fig. 3 D). Taken together, the results shown in Fig. 3 suggest that the cysteine in position 428 plays an important role in the current blockage induced by Cu/P application, although additional cysteines other than C428 are also likely involved. This observation indicates that the C428 residues readily form disulfide bonds and must be close to each other within the intracellular mouth of the pore. In other words, the C_α of cysteines 428 must be separated by 10 Å or less, as shown in Fig. 8. This is in agreement with the observed intracellular Cd^{2+} blockage in the w.t. channel (Fig. 2 D).

Cd^{2+} ions usually bind to more than one cysteine (Krovetz et al., 1997); therefore, the Cd^{2+} blockage indicates that cysteines in position 428 are close enough to cooperatively form a Cd^{2+} binding site.

Ion selectivity

K^+ and CNG channels displayed a ring of negatively charged residues in their extracellular vestibule (for K^+ channels, see Doyle et al., 1998 on the KcsA channel; for CNG channels, see Root and MacKinnon, 1993, and Eismann et al., 1994, on the α-subunit of bovine rod channel). As shown in Fig. 1 A, SpHCN and hHCN4 channels, instead, had a positively charged residue at the homologous location, i.e., a lysine and an arginine, respectively. In this work, a possible role as "intermediate" ion selectivity was examined for lysine 433 in the SpHCN channel. Mutants K433D and K433E, which should mimic highly selective K^+ channels (see Fig. 1 A), were engineered. However, it
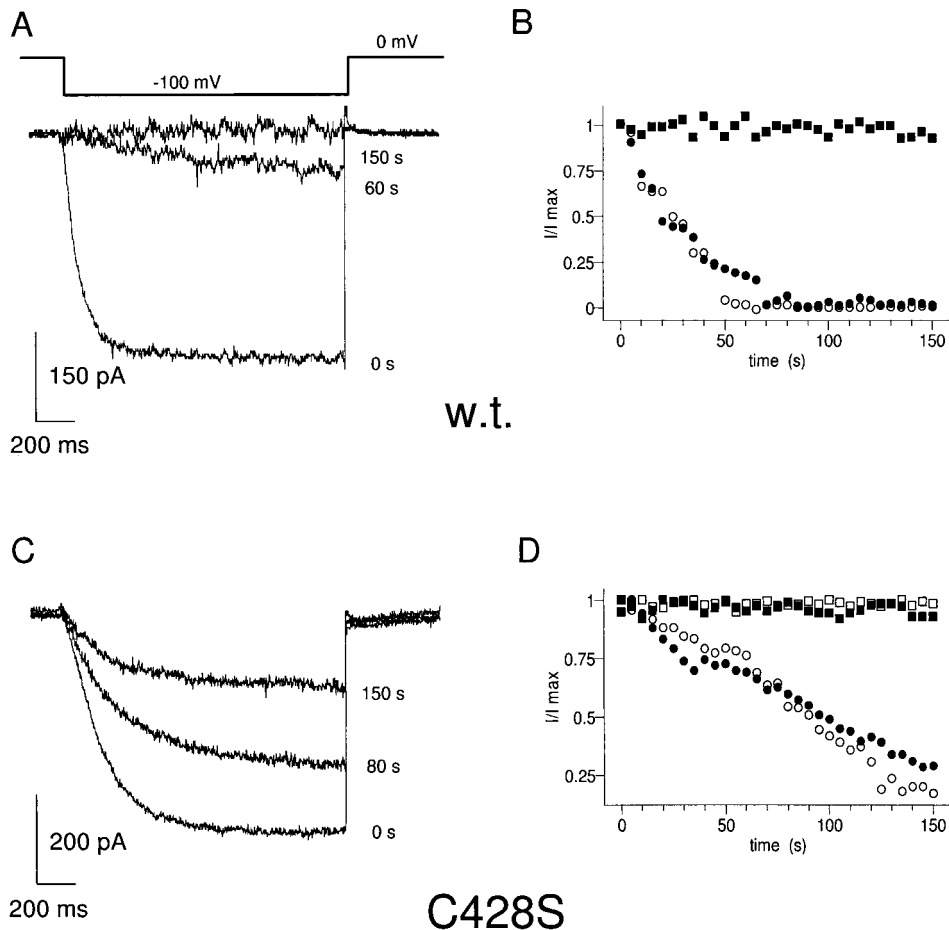
FIGURE 3   Intracellular effect of copper phenanthroline on the w.t. (*A*) and C428S (*C*) I_h currents. Currents were elicited as in Fig. 1 *B*. First, I_h currents were activated with a hyperpolarizing pulse from 0 to -100 mV, in the absence of Cu/P (copper phenanthroline) and in the presence of 1 mM cAMP in the bath solution (0 s in *A* and *C*). Then, the effect of Cu/P was tested by continuously bathing the intracellular side of the membrane patch in a solution containing 1.5:5 μM Cu/P and 1 mM cAMP, and applying the same hyperpolarizing pulse as above every 5 s. Shown in *A* and *C* are current traces recorded after 60 (or 80) and 150 s. Data are representative of five experiments. Time courses of Cu/P block for the w.t. and C428S mutant channel are shown in *B* and *D*, respectively. In both panels, data shown are taken from two independent experiments (indicated by *open* and *filled symbols*). Squares indicate control experiments (i.e., performed as in *A* and *C* but without Cu/P addition). In panel *B*, data for control are relative to one single representative experiment, as no current rundown was ever observed for the w.t. channel in normal conditions, even after prolonged activation.

was impossible to determine the ion selectivity of these mutants. While no expression was detected for K433E, a small I_h current from K433D was occasionally observed but it was not possible to perform all the experiments required to reliably determine ion selectivity (an I_h current was observed only in two instances of >63 patches excised from 22 oocytes). Therefore, mutant K433Q was prepared, in which the positive charge of the lysine was neutralized by substitution with glutamine. An interesting feature of this channel is that the K433Q mutation significantly modified the time course of the I_h activation. As shown in Fig. 4 *B*, recordings obtained when the voltage command was stepped from 0 mV to negative voltages exhibited an unusual profile with an initial activation followed by a current decline, never observed in the w.t. channel (Fig. 4 *A*).

Subsequently, the K433Q conductance was also assessed. The steady-state activation of the conductance underlying

the I_h current for the w.t. and K433Q mutant channels measured in inside-out configuration is shown in Fig. 4 *C* (*filled* and *open symbols*, respectively). The w.t. conductance was half-activated at ~ -45 mV, in agreement with previous reports (Gauss et al., 1998). In contrast, the half-activation of the mutant channel K433Q occurred at more negative voltages, around -95 mV.

The ionic selectivity of mutant channel K433Q was then studied, in inside-out membrane patches, analyzing tail currents at their peak (see Gauss et al., 1998). Given the rundown of the I_h current in this mutant (discussed below), the reversal potential for different ions was studied in different patches. Fig. 5 *A* shows current recordings from the mutant channel K433Q, when intracellular K^+ only was present (K^+) and when it was partly replaced with Na^+ (Na^+) or Li^+ (Li^+). Partial replacement was necessary because the SpHCN channel, like other HCN channels, does
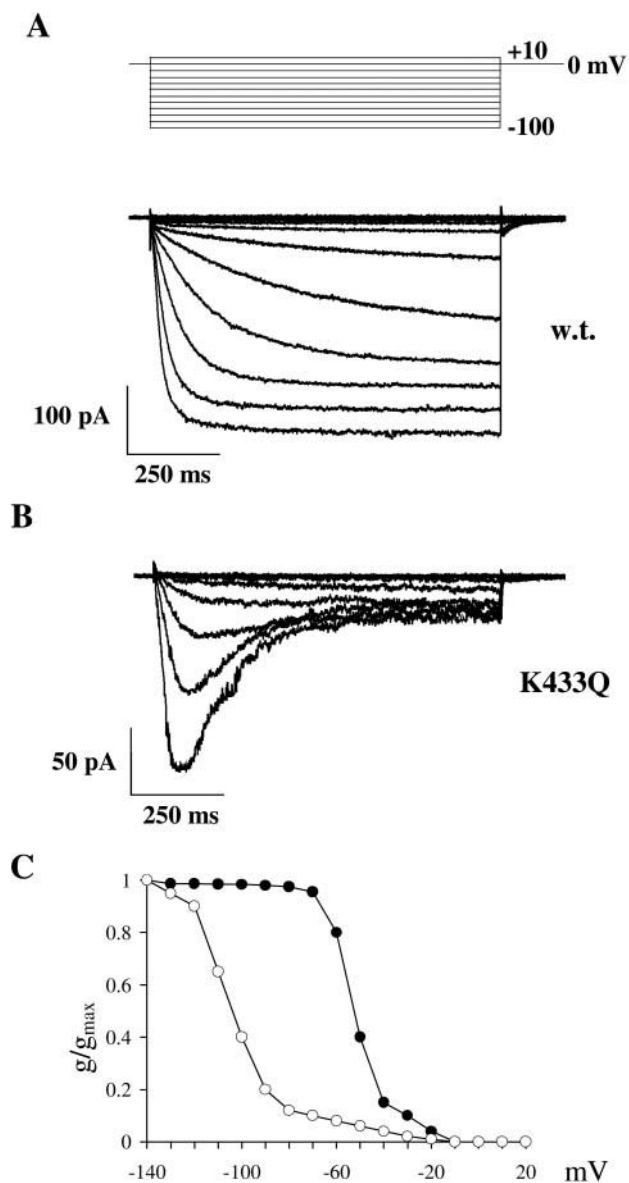
FIGURE 4   Current-voltage relation of the w.t. and K433Q mutant channels. (*A*) Current recordings from inside-out patches for the w.t. channel. Voltage steps are from −100 to +10 mV in 10 mV steps, in the presence of 1 mM cAMP in the intracellular medium. Traces are representative of 10 experiments. (*B*) Current recordings from inside-out patches for the K433Q mutant channel. Voltage steps as in *A*. I_h currents in *A* and *B* were isolated as shown in Fig. 1 *B*. Traces are representative of 10 experiments. (*C*) Neutralization of lysine 433 shifts the half-activation by ∼50 mV. Normalized conductances underlying I_h currents for the w.t. channel at the steady state, taken from panel *A* (*filled symbols*), and for the K433Q mutant channel at the peak of its activation and before development of inactivation, taken from panel *B* (*open symbols*). Conductances are relative to experiments in which voltage steps were applied from −140 to +10 mV in 10 mV steps, in the presence of 1 mM cAMP in the intracellular medium. Conductance values are normalized to g_{max} (i.e., at −140 mV).

not conduct in the absence of K^+ ions (see Gauss et al., 1998). The relationship between the amplitude of tail currents and the membrane voltage for the mutant channel

K433Q is shown in Fig. 5 *B*. The reversal potential was 14.5 ± 2.5 mV for Na^+ (four patches) and 24.5 ± 6.5 mV for Li^+ (six patches). These values are similar to those obtained for the w.t. channel: 16.9 mV for Na^+ and 20.6 mV for Li^+ (Gauss et al., 1998).

The dependence of the K433Q current on bath cAMP is also very similar to that of the w.t. channel. The I_h currents activated by different concentrations of cAMP (0.0025, 0.01, 0.1, and 1 mM) in this mutant are shown in Fig. 5 *C*. These different cAMP concentrations were tested within <10 s to minimize the intrinsic rundown of the K433Q I_h current (discussed below). A comparison with similar data obtained from the w.t. SpHCN channel (illustrated in Fig. 5 *D*) does not reveal any significant difference. Taken together, these results indicate that despite different time courses of activation and different conductance, the ionic selectivity and cyclic nucleotide sensitivity of the K433Q mutant is very similar to that of the w.t. channel. This suggests that the ion selectivity of the SpHCN channel does not depend significantly on the presence of a positive charge at location 433.

As mentioned previously, the I_h current observed in inside-out patch recordings from mutant K433Q exhibited a significant rundown. The I_h current activated at −100 mV declined within 1 min by ∼50% following membrane excision from the oocyte and perfusion with 1 mM cAMP on the intracellular side of the membrane (Fig. 6, *A* and *B*). This rundown was reduced when 2 mM of the reducing agent DTT was added to the intracellular medium (data not shown). This suggests that this behavior is due to the formation of sulfhydryl bridges between cysteines at position 428 located at the inner mouth of the channel pore, which come in closer contact with each other following replacement of lysine 433 with glutamine. To further evaluate this possibility, the double mutant C428S+K433Q was constructed. Indeed, no significant rundown in the C428S+K433Q mutant was observed, even during prolonged time course (Fig. 6, *C* and *D*). This result confirms that the presence of C428 is important for a development of observed rundown.

Lysine 433 does not mediate the blocking effect of large extracellular anions

Large anions are known to reduce or block the I_h current from the extracellular side in both native (Frace et al., 1992) and heterologously expressed (Santoro et al., 1998) HCN channels. Here, we report a similar behavior in the w.t. SpHCN channel.

As shown in Fig. 7 *A*, when the external Cl^- was replaced with larger anions, such as acetate, glutamate, and sulfate during outside-out recordings, the I_h current was almost completely abolished. On the contrary, during inside-out recordings, the substitution of intracellular Cl^- with acetate, glutamate, or sulfate modified the time course of the I_h
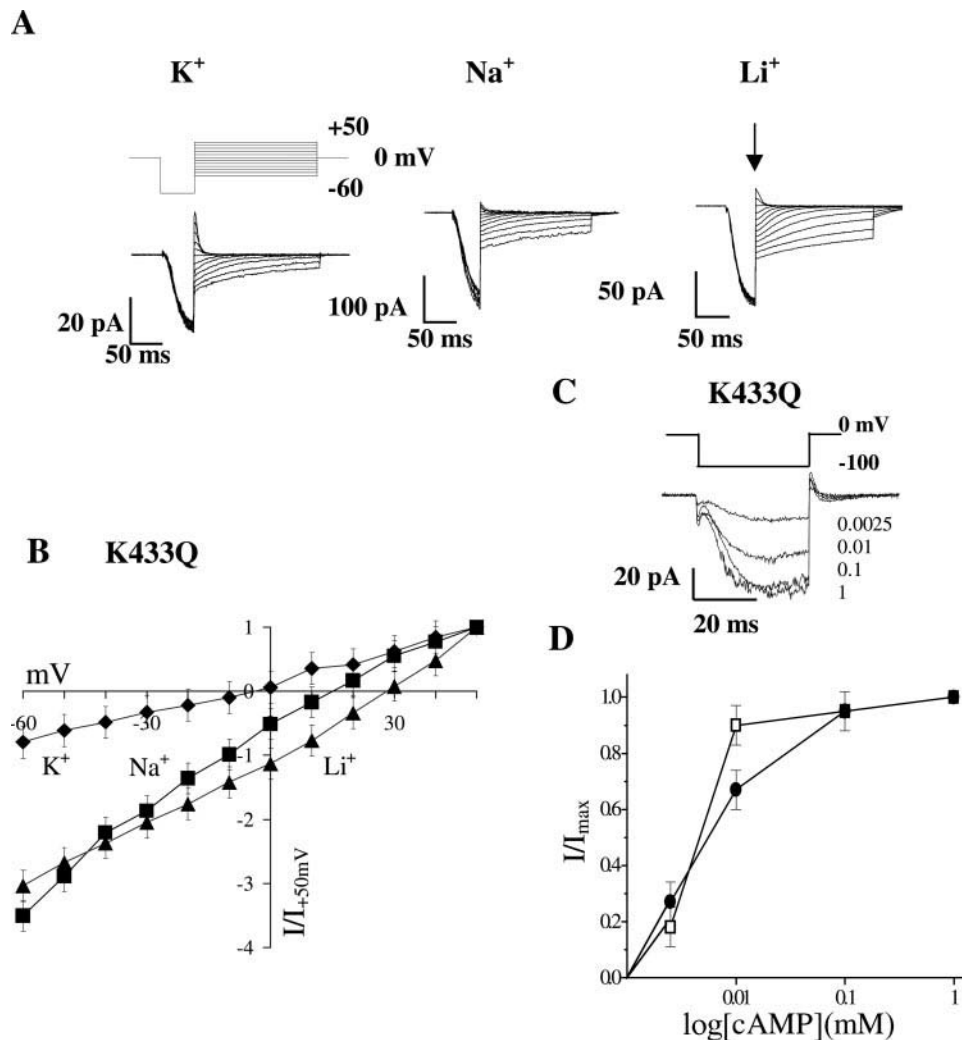
FIGURE 5   Ion selectivity and cyclic nucleotide sensitivity of mutant channel K433Q. (*A*) Current recordings with different cations for mutant channel K433Q in inside-out configuration. Solutions on the intracellular side of the membrane contained: (K^+) 150 mM KCl; (Na^+) 50 mM KCl + 100 mM NaCl; (Li^+) 50 mM KCl + 100 mM LiCl. The protocol, from a holding potential of 0 mV, consisted in a hyperpolarizing step to −120 mV, lasting 50 ms, followed by voltage steps from +50 to −60 mV, in 10 mV intervals. The *arrow* indicates the time when the instantaneous current-voltage relationship was taken. I_h currents were isolated as shown in Fig. 1 *B*. Current recordings for mutant channel K433Q were collected in <10 s, during which the rundown of the I_h current was only ~10%. Each trace shown is representative of four different experiments. (*B*) Instantaneous current-voltage relationship at the peak of the tail current from experiments as in *A*. Currents were normalized to the tail current measured at +50 mV. Each point is the average of four different experiments. Vertical bars indicate standard deviation. (*C*) The cAMP sensitivity of the K433Q channel. I_h currents were activated by different concentrations of cAMP (0.0025, 0.01, 0.1, and 1 mM). (*D*) A comparison of cAMP sensitivity of the K433Q channel (*open symbols*) with that of the w.t. channel (*filled symbols*). Data for the mutant channel K433Q and for the w.t. channel were obtained from eight and four different experiments, respectively. Currents were normalized to the current flowing in the presence of 1 mM cAMP. Vertical bars indicate standard deviation. The determination of cAMP sensitivity for mutant K433Q occurred in <10 s, during which the rundown of the I_h current was <10%. Voltage steps as in Fig. 1 *B*.

current, but did not reduce its amplitude (Fig. 7 *B*). The effect of aspartate was also tested, and was comparable to that of the other anions (data not shown). Because the positively charged lysine in position 433 appears to face the extracellular side of the channel (see Fig. 2 *B*), this residue is a good candidate for mediating the observed blocking effect. However, the mutant channel K433Q was reversibly blocked by extracellular anions (Fig. 7 *C*). This indicates that lysine 433 is not involved in this type of blockade of the w.t. SpHCN channel.

DISCUSSION

The results described in this paper provide a preliminary determination of the pore topology of the SpHCN channel, necessary to understand its functional properties, such as ion selectivity, which is intermediate between that of selective K^+ channels and of nonselective CNG channels. Based mainly on the high homology among HCN, CNG, and K^+ channels (see Fig. 1 *A*), the pore region of the SpHCN channel is presumed to be built by the polypeptidic frag-
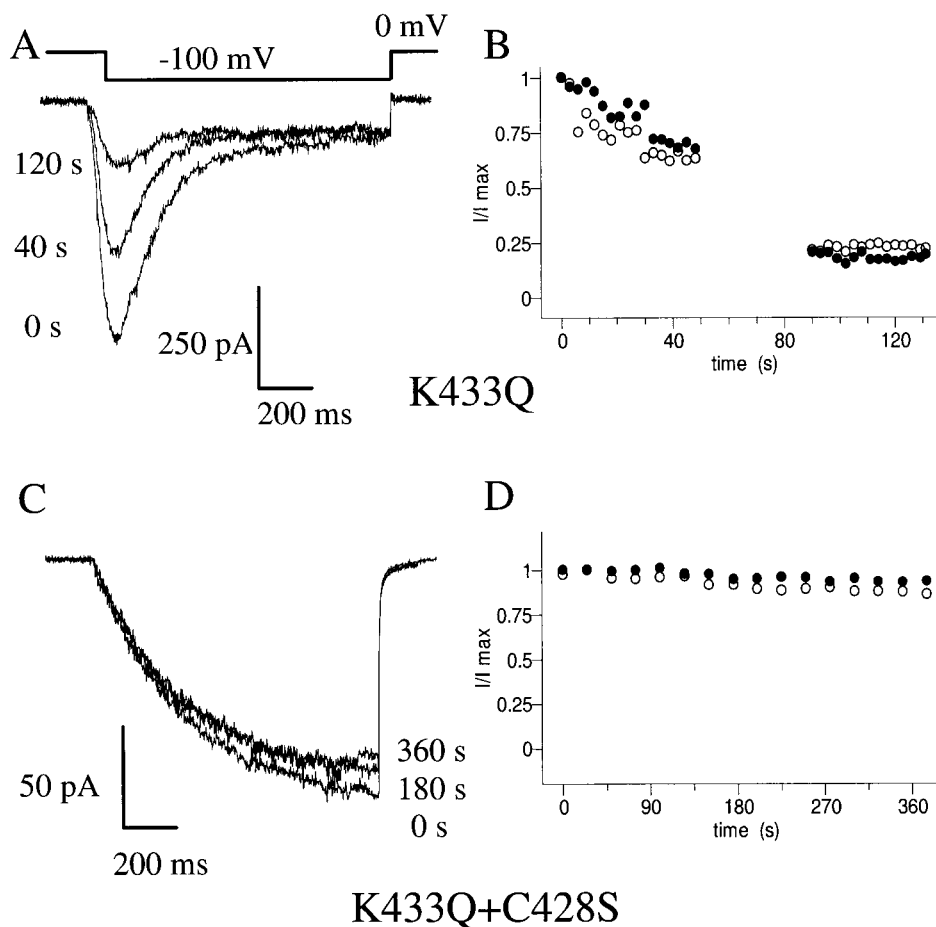
FIGURE 6 Current rundown in mutant channels K433Q and C428S+K433Q. I_h currents were elicited in mutant channels K433Q and C428S+K433Q (*A* and *C*, respectively) by applying a hyperpolarizing step of -100 mV lasting 1 s to inside-out patches of membrane every 2 s, in the presence of 1 mM cAMP in the intracellular medium. The protocol was applied continuously, and the superimposed traces shown were recorded immediately after patch excision (0 s) and at later times (40 and 120 s for the K433Q channel in *A*, 180 and 360 s for the C428S+K433Q channel in *C*). Data are representative of four different experiments. Current kinetics for mutant channels K433Q and C428S+K433Q are shown in panels *B* and *D*, respectively. Data were taken from two independent experiments (indicated by *open* and *filled symbols*).

ment connecting its fifth and sixth hydrophobic regions, i.e., amino acids from 416 to 438 (see Fig. 1 *A*). This stretch of residues contains several conserved features of K$^+$ channels (Heginbotham et al., 1994), mainly the GYG motif. In the present study, an extensive mutational analysis of pore-forming residues was performed to investigate their physical location and functional properties.

The substituted-cysteine accessibility method (SCAM; Karlin and Akabas, 1998) was used to characterize the topology of pore residues. The blocking effect of intracellular Cd^{2+} on the w.t. SpHCN current (Fig. 2 *D*), and the absence of this effect when Cd^{2+} is applied extracellularly (Fig. 2 *A*), as well as the behavior of mutant C428S (Fig. 2 *E*), firmly establish that cysteine in position 428 faces the cytoplasmic side of the channel pore, and constitutes a binding site for Cd^{2+}. The current inhibition in mutant K433C and F434C by extracellular Cd^{2+} (Fig. 2, *B* and *C*) indicates that lysine 433 and phenylalanine 434 face the

extracellular vestibule. Taken together, these data indicate that the stretch of residues CIGYGKF, including the K$^+$ channel selectivity filter GYG, penetrates the membrane and connects the intracellular and extracellular vestibules of the pore, with residues IGYG forming the walls of the inner pore of the SpHCN channel.

Given the very high sequence homology in the pore regions of the SpHCN channel and all other cloned HCN channels, these proteins are all likely to share the same pore topology. These features are illustrated in the model of the pore of the SpHCN channel, shown in Fig. 8. This model, which is based on homology modeling with the crystal structure of the KcsA K$^+$ channel (Zhou et al., 2001), has been built recently (A. Giorgetti, P. Mistrik, P. Carloni, and V. Torre, manuscript in preparation). We conclude from our data that residues from cysteine 428 to phenylalanine 434 form the pore walls. Residues from 415 to 426 are likely to form the presumed pore helix.
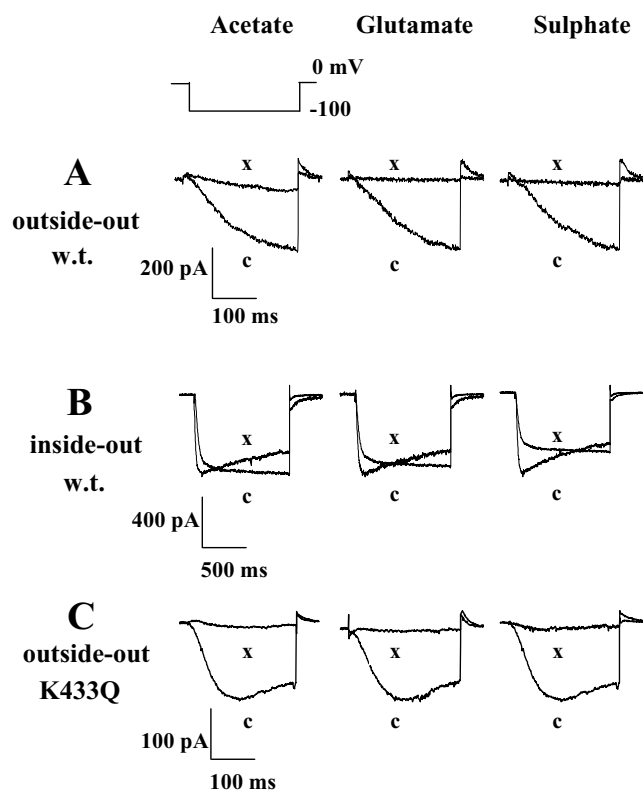
Acetate   Glutamate   Sulphate

A
outside-out
w.t.

B
inside-out
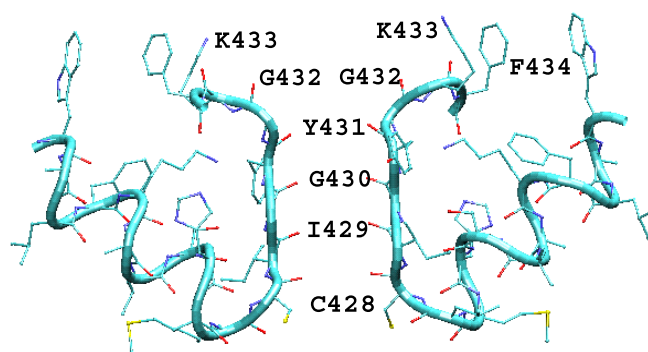**w.t.**

C
outside-out
K433Q

FIGURE 8   Model of the SpHCN channel pore region. Two monomers of the four present are displayed for the sake of clarity. The model is derived by homology with the 3D crystal structure of the KcsA channel (Zhou et al., 2001). Amino acids 417 to 427 are supposed to form a pore helix. This model bears structural features consistent with the experimental data presented in this work: the location of phenylalanine 434 and lysine 433 near the extracellular vestibule and the location of the cysteine 428 in the opening of the intracellular mouth. The C_α of opposing cysteines 428 are separated by ~9 Å and the C_α of adjacent cysteines are ~6.5 Å apart. The homology model suggests that the selectivity filter GYG broadens at the extracellular mouth and that the narrowest part of the pore is formed by residues from cysteine 428 to tyrosine 431. The presented model (A. Giorgetti, P. Mistrik, P. Carloni, and V. Torre, manuscript in preparation) was built using the MODELLER (Sali and Blundell, 1993) program.

FIGURE 7   The effect of substituting external chloride with larger anions in the SpHCN channel. KCl was substituted with potassium acetate (*left*), potassium glutamate (*middle*), or potassium sulfate (*right*). In all panels, control currents (indicated by c) and anion-substituted currents (indicated by x) are superimposed. Traces are representative of three different experiments. (*A*) Replacement of extracellular chloride with larger anions in w.t. channel. Current recordings obtained from outside-out patch-clamp. Voltage steps as in Fig. 1 *C*. (*B*) Replacement of intracellular chloride with larger anions in the w.t. channel; current recordings were obtained with inside-out patch-clamp. Voltage step as in Fig. 1 *B*. (*C*) Replacement of extracellular chloride with larger anions in the K433Q mutant channel. Current recordings were obtained with outside-out patch-clamp. Voltage steps as in Fig. 1 *C*.

After establishing the topology of the SpHCN channel pore, its particular ion selectivity was addressed. SpHCN has "intermediate" ion selectivity between selective K^+ channels and nonselective CNG channels. An important determinant of high selectivity of K^+ channels is a negatively charged residue following the GYG selectivity filter (Chapman et al., 2001). Because the SpHCN channel and other HCN channels have a unique positively charged residue in the homologous position, i.e., lysine 433 in the extracellular vestibule, a possible involvement of this residue in the SpHCN ion selectivity was investigated. Mutant K433Q, in which the positive charge of the lysine is neutralized by substitution with glutamine, was constructed. Physical properties of this mutant, i.e., time course of activation (Fig. 4 *B*), conductance (Fig. 4 *C*), ion selectivity (Fig. 5 *B*), and dependence of the I_h current on bath cAMP concentration (Fig. 5 *D*) taken together indicate that despite

different time course of activation and different conductance, the ion selectivity and cyclic nucleotide sensitivity of the K433Q mutant are very similar to those of the w.t. channel. This suggests that the positive charge of lysine 433 does not contribute to the selectivity of the SpHCN channel among monovalent alkali cations, nor to its sensitivity to cyclic nucleotides. Because K433 alone cannot explain the ion selectivity of SpHCN, it is more likely that the intermediate selectivity depends on global geometrical properties of the pore, such as its radius, resulting from a cooperative action of many residues, rather than on specific electrostatic properties of individual residues (Laio and Torre, 1999).

The blockade of the SpHCN channel by extracellular anions reported previously for both native (Frace et al., 1992) and heterologously expressed (Santoro et al., 1998) HCN channels was also investigated. The I_h current from the w.t. SpHCN channel was found to be blocked extracellularly (Fig. 7 *A*), but not intracellularly (Fig. 7 *B*), by large anions such as acetate, glutamate, and sulfate, in accordance with all data reported above. The positive charge of lysine 433 makes it an ideal candidate for a residue responsible for this blockade of SpHCN. However, the mutant K433Q also exhibits a significant block (Fig. 7 *C*). Therefore, lysine 433 does not mediate the blocking effect of extracellular large anions in the SpHCN channel.

However, lysine in position 433 might be a key structural element in the pore architecture. We propose that K433 plays an important role in keeping apart the subunits that

form the presumed tetrameric channel pore, so that the cysteines in the inner ring (position 428) cannot form disulfide bridges. This conclusion stems from our observations that substitution of lysine 433 with glutamine leads to the current rundown shown in Fig. 6 *A*, which can be overrun by applying a reducing reagent such as DTT (data not shown). A cooperative action between K433 and C428 was confirmed by construction of the C428S+K433Q double mutant, in which no current rundown was observed (Fig. 6 *B*).

The spatial proximity of the cysteines in the SpHCN channel pore was also confirmed by exposure of the intracellular vestibule to a mild oxidative agent such as copper phenanthroline (Cu/P). Its addition resulted in a rapid I_h current decline (Fig. 3 *A*), likely due to the formation of disulfide bridges. This current block is not reversible and exhibits exponential decay kinetics with a time constant of 25 ± 4 s (Fig. 3 *B*). The intracellular ring of cysteines may constitute a modulatory mechanism of channel gating and an excellent sensor of the redox potential inside the cell. These characteristics may be common features to all HCN channels.

REFERENCES

Becchetti, A., and K. Gamel. 1999. The properties of cysteine mutants in the pore region of cyclic nucleotide-gated channels. *Pflügers Arch.* 438:587–596.

Becchetti, A., K. Gamel, and V. Torre. 1999. Cyclic nucleotide-gated channels: pore topology studied through the accessibility of reporter cysteines. *J. Gen. Physiol.* 114:377–392.

Becchetti, A., and P. Roncaglia. 2000. Cyclic nucleotide-gated channels: intra and extracellular accessibility to Cd^{2+} of substituted cysteine residues within the P-loop. *Eur. J. Physiol.* 440:556–565.

Brown, H. F., and W. K. Ho. 1996. The hyperpolarization-activated inward channel and cardiac pacemaker activity. *In* Molecular Physiology and Pharmacology of Cardiac Ion Channels and Transporters. M. Morad, S. Ebashi, W. Trautwein, and Y. Kurachi, editors. Kluwer, Dordrecht, The Netherlands. 17–30.

Capovilla, M., A. Caretta, L. Cervetto, and V. Torre. 1983. Ionic movements through light-sensitive channels of toad rods. *J. Physiol.* 343:295–310.

Chapman, M. L., H. S. Krovetz, and A. M. VanDongen. 2001. GYGD pore motifs in neighboring potassium channel subunits interact to determine ion selectivity. *J. Physiol.* 530:21–33.

Clapham, D. E. 1998. Not so funny anymore: pacing channels are cloned. *Neuron.* 21:5–7.

DiFrancesco, D. 1993. Pacemaker mechanisms in cardiac tissues. *Annu. Rev. Physiol.* 55:455–472.

Doyle, D. A., J. Morais Cabral, R. A. Pfuetzner, A. Kuo, J. M. Gulbis, S. L. Cohen, B. T. Chait, and R. MacKinnon. 1998. The structure of the potassium channel: molecular basis of K^+ conduction and selectivity. *Science.* 280:69–77.

Eismann, E., F. Müller, S. Heinemann, and U. B. Kaupp. 1994. A single negative charge within the pore region of a cGMP-gated channel controls rectification, Ca^{2+} blockage, and ionic selectivity. *Proc. Natl. Acad. Sci. U.S.A.* 91:1109–1113.

Fain, G. L., F. N. Quandt, B. L. Bastian, and H. M. Gerschenfeld. 1978. Contribution of a cesium-sensitive conductance increase to the rod photoresponse. *Nature.* 272:466–469.

Fesenko, E. E., S. S. Kolesnikov, and A. L. Lyubarsky. 1985. Induction by cyclic GMP of cationic conductance in plasma membrane of retinal rod outer segment. *Nature.* 313:310–313.

Flynn, G. E., and W. N. Zagotta. 2001. Conformational changes in S6 coupled to the opening of cyclic nucleotide-gated channels. *Neuron.* 30:689–698.

Frace, A. M., F. Maruoka, and A. Noma. 1992. Control of the hyperpolarization-activated cation current by external anions in rabbit sinoatrial node cells. *J. Physiol.* 453:307–318.

Gauss, R., and R. Seifert. 2000. Pacemaker oscillations in heart and brain: a key role for hyperpolarization-activated cation channels. *Chronobiol. Int.* 17:453–469.

Gauss, R., R. Seifert, and U. B. Kaupp. 1998. Molecular identification of a hyperpolarization-activated channel in sea urchin sperm. *Nature.* 393:583–587.

Gordon, S. E., and W. N. Zagotta. 1995. A histidine residue associated with the gate of the cyclic nucleotide-activated channels in rod photoreceptors. *Neuron.* 14:177–183.

Halliwell, J. V., and P. R. Adams. 1982. Voltage-clamp analysis of muscarinic excitation in hippocampal neurons. *Brain. Res.* 250:71–92.

Hamill, O. P., A. Marty, E. Neher, B. Sakmann, and F. J. Sigworth. 1981. Improved patch-clamp technique for high resolution current recording from cells and cell-free membrane patches. *Pflugers Arch.* 391:85–100.

Heginbotham, L., Z. Lu, T. Abramson, and R. MacKinnon. 1994. Mutations in the K^+ channel signature sequence. *Biophys. J.* 66:1061–1067.

Ho, W. K., H. F. Brown, and D. Noble. 1994. High selectivity of the i_f channels to Na^+ and K^+ in rabbit isolated sinoatrial node cells. *Pflügers Arch.* 426:68–74.

Humphrey, W., A. Dalke, and K. Schulten. 1996. VMD visual molecular dynamics. *J. Mol. Graph.* 14:33–38.

Ishii, T. M., M. Takano, L.-H. Xie, A. Noma, and H. Ohmori. 1999. Molecular characterization of the hyperpolarization-activated cation channel in rabbit heart sinoatrial node. *J. Biol. Chem.* 274:12835–12839.

Karlin, A., and M. H. Akabas. 1998. Substituted-cysteine accessibility method. *In* Methods in Enzymology. P. M. Conn, editor. Academic Press, San Diego. 123–145.

Kaupp, U. B., T. Niidome, T. Tanabe, S. Terada, W. Bönigk, W. Stuhmer, N. J. Cook, K. Kangawa, H. Matsuo, and T. Hirose. 1989. Primary structure and functional expression from complementary DNA of the rod photoreceptor cyclic GMP-gated channel. *Nature.* 342:762–766.

Krieger, J., J. Strobel, A. Vogl, W. Hanke, and H. Breer. 1999. Identification of a cyclic nucleotide- and voltage-activated ion channel from insect antennae. *Insect Biochem. Mol. Biol.* 29:255–267.

Krovetz, H. S., H. M. A. VanDongen, and A. M. J. VanDongen. 1997. Atomic distance estimates from disulfides and high-affinity metal-binding sites in a K^+ channel pore. *Biophys. J.* 72:117–126.

Kubo, Y., M. Yoshimichi, and S. H. Heinemann. 1998. Probing pore topology and conformational changes of Kir2.1 potassium channels by cysteine scanning mutagenesis. *FEBS Lett.* 435:69–73.

Kurz, L. L., R. D. Zuhlke, H.-J. Zhang, and R. H. Joho. 1995. Side-chain accessibilities in the pore of a K^+ channel probed by sulfhydryl-specific reagents after cysteine-scanning mutagenesis. *Biophys. J.* 68:900–905.

Laio, A., and V. Torre. 1999. Physical origin of selectivity in ionic channels of biological membranes. *Biophys. J.* 76:129–148.

Ludwig, A., X. Zong, M. Jeglitsch, F. Hofmann, and M. Biel. 1998. A family of hyperpolarization-activated mammalian cation channels. *Nature.* 393:587–591.

Ludwig, A., X. Zong, J. Stieber, R. Hullin, F. Hofmann, and M. Biel. 1999. Two pacemaker channels from human heart with profoundly different activation kinetics. *EMBO J.* 18:2323–2329.

Marx, T., G. Gisselmann, K. F. Stoertkuhl, B. T. Hovemann, and H. Hatt. 1999. Molecular cloning of a putative voltage- and cyclic nucleotide-gated ion channel present in the antennae and eyes of *Drosophila melanogaster*. *Invert. Neurosci.* 4:55–63.

Miledi, R., and I. Parker. 1984. Chloride currents induced by injection of Ca^{2+} into *Xenopus* oocytes. *J. Physiol. (Lond.).* 357:173–183.

Nizzari, M., F. Sesti, M. T. Giraudo, C. Virginio, A. Cattaneo, and V. Torre. 1993. Single-channel properties of cloned cGMP-activated channels from retinal rods. *Proc. R. Soc. Lond. B.* 254:69–74.

Pape, H. C. 1996. Queer current and pacemaker: the hyperpolarization-activated cation current in neurons. *Annu. Rev. Physiol.* 58:299–327.

Pongs, O., N. Kecskemethy, R. Müller, I. Krah-Jentgens, A. Baumann, H. H. Kiltz, I. Canal, S. Llamazares, and A. Ferrus. 1988. *Shaker* encodes a family of putative potassium channel proteins in the nervous system of *Drosophila*. *EMBO J.* 7:1087–1096.

Root, M. J., and R. MacKinnon. 1993. Identification of an external divalent cation-binding site in the pore of a cGMP-activated channel. *Neuron.* 11:459–466.

Sali, A., and T. L. Blundell. 1993. Comparative protein modeling by satisfaction of spatial restraints. *J. Mol. Biol.* 234:779–815.

Santoro, B., S. G. N. Grant, D. Bartsch, and E. R. Kandel. 1997. Interactive cloning with the SH3 domain of N-src identifies a new brain-specific ion channel protein, with homology to Eag and cyclic nucleotide-gated channels. *Proc. Natl. Acad. Sci. U.S.A.* 94:14815–14820.

Santoro, B., D. T. Liu, H. Yao, D. Bartsch, E. R. Kandel, S. A. Siegelbaum, and G. R. Tibbs. 1998. Identification of a gene encoding a hyperpolarization-activated pacemaker channel of brain. *Cell.* 93:717–729.

Santoro, B., and G. R. Tibbs. 1999. The HCN gene family: molecular basis of the hyperpolarization-activated pacemaker channels. *Ann. NY Acad. Sci.* 868:741–764.

Seifert, R., A. Scholten, R. Gauss, A. Mincheva, P. Lichter, and U. B. Kaupp. 1999. Molecular characterization of a slowly gating human hyperpolarization-activated channel predominantly expressed in thalamus, heart, and testis. *Proc. Natl. Acad. Sci. U.S.A.* 96:9391–9396.

Sesti, F., E. Eismann, U. B. Kaupp, M. Nizzari, and V. Torre. 1995. The multi-ion nature of the cGMP-gated channel from vertebrate rods. *J. Physiol. (Lond.).* 487:17–36.

Shi, W., R. Wymore, H. Yu, J. Wu, R. T. Wymore, Z. Pan, R. B. Robinson, J. E. Dixon, D. McKinnon, and I. S. Cohen. 1999. Distribution and prevalence of hyperpolarization-activated cation channel (HCN) mRNA expression in cardiac tissues. *Circ. Res.* 85:1–16.

Vaccari, T., A. Moroni, M. Rocchi, L. Gorza, M. E. Bianchi, M. Beltrame, and D. DiFrancesco. 1999. The human gene coding for HCN2, a pacemaker channel of the heart. *Biochim. Biophys. Acta.* 1446:419–425.

Wollmuth, L. P., and B. Hille. 1992. Ionic selectivity of I_h channels of rod photoreceptors in tiger salamanders. *J. Gen. Physiol.* 100:749–765.

Yellen, G., D. Sodickson, T.-Y. Chen, and M. E. Jurman. 1994. An engineered cysteine in the external mouth of a K^+ channel allows inactivation to be modulated by metal binding. *Biophys. J.* 66: 1068–1075.

Zhou, Y., J. H. Morais-Cabral, A. Kaufman, and R. Mackinnon. 2001. Chemistry of ion coordination and hydration revealed by a K^+ channel-Fab complex at 2.0 Å resolution. *Nature.* 414:43–48.